Hyperbolic tangle surgeries and nested links

JOHN HARNOIS

HAYLEY OLSON

ROLLAND TRAPP

Changes to gluing patterns for fully augmented links are shown to result in generalized fully augmented links. The first changes considered result in 4–tangle surgeries on hyperbolic fully augmented links that produce hyperbolic generalized fully augmented links. These surgeries motivate the definition of nested links, and a characterization of hyperbolic nested links is given. Finally, the geometry of nested links is compared to that of fully augmented links.

1 Introduction

This paper compares fully augmented links to generalized fully augmented links. Fully augmented links (FALs) are obtained from a twist-reduced link diagram by placing trivial components (called "crossing circles") around each twist region, then eliminating all full twists. For FALs, one considers traditional twist regions involving only two strands. Generalized fully augmented links (GFALs) are obtained similarly, but allow for more than two strands per twist region. These classes of links are appealing because of their geometric simplicity and for the fact that, through Dehn filling, they provide geometric insight into hyperbolic links in general.

Adams introduced the process of augmenting a link with a crossing circle in [2], where he showed that augmenting (nontorus) alternating links always produced hyperbolic links. A fully augmented link occurs when *all* twist regions are augmented. The particularly tractable geometry of fully augmented links is outlined by Purcell in [12]. One feature is that FALs have a standard cell decomposition, described in the appendix of Lackenby [9], which shows they can be built by gluing two identical ideal right-angled polyhedra. This cell decomposition shows that all fully augmented link complements contain reflection surfaces — totally geodesic surfaces which are fixed point sets of a reflection on the link complement. Purcell also shows that the polyhedral decomposition

is canonical (à la Epstein and Penner [5]), and further uses it to determine cusp shapes of fully augmented links. Moreover, the concrete nature of this cell decomposition has been used by a variety of authors to further our understanding of hyperbolic links; see [12] for an excellent summary.

Generalized fully augmented links were considered by Purcell [10; 11] and by Futer, Kalfagianni and Purcell [7], where they were used to study the geometry of hyperbolic links with lots of twists. In particular, GFALs have provided bounds on volumes and on lengths of geodesics, and they relate the geometry of a link to its diagram. Adams, in [4], generalized his results of [2] and showed that generalized augmented alternating links are hyperbolic.

We see that FALs and GFALs have had similar applications, so the comparison between them warrants further attention. One similarity, as a result of Adams' work [2; 4], is that starting with an alternating link, fully augmenting yields a hyperbolic link in either case. Another, as described in [11], is that both FALs and GFALs admit reflection surfaces, the presence of which allowed Purcell to determine sufficient conditions on when Dehn fillings produced hyperbolic manifolds. Thirdly, both FALs and GFALs have been used to provide volume bounds for hyperbolic links; see [9; 4; 11] for example.

There are significant differences between FALs and GFALs as well. Each crossing circle in a FAL bounds a totally geodesic 3–punctured sphere; see Adams [1]. Crossing circles in a GFAL bound n–punctured spheres which need not be totally geodesic; see [4; 10]. A related difference is that in a FAL, adding a half twist to a crossing circle always preserves hyperbolicity, while the same is not true in the case of GFALs. There are significant differences between the standard cell decomposition of a FAL and its natural generalization to GFALs as well. In particular, the standard cell decomposition of a FAL leads to a triangulation which allows one to apply Andreev's theorem to prove hyperbolicity. As noted in [12], one loses the triangulation on passing to GFALs, hence the application of Andreev's theorem, and the hyperbolic geometry of a GFAL is not as clean.

In this paper, we take a closer look at the cell decomposition of FALs and their description as the identification of two right-angled ideal polyhedra. In Section 2, we review the necessary background and develop appropriate terminology. The right-angled polyhedra $P_\pm$, together with their gluing patterns, are described in detail. Section 3 considers slightly more general gluing patterns on $P_\pm$, and Theorem 3.2 shows they result in complete hyperbolic manifolds. The manifolds that result from these more

general gluing patterns always contain reflection surfaces. In Section 4, tangles in a FAL involving consecutive crossing circles are considered; see Figure 4. It is shown that certain surgeries on those tangles correspond to slightly altered gluing patterns which result in complete hyperbolic manifolds. These surgeries transform a FAL into a GFAL built from the same, or related, polyhedra. This fact is demonstrated by using a nonstandard cell decomposition on the GFAL. The nonstandard cell decomposition motivates the definition of *nested links* in Section 5. Nested links are GFALs that are similar to FALs in several ways. For nested links, Andreev's theorem can be used to prove they are hyperbolic, they can be characterized combinatorially by generalizing Purcell's *dimer* characterization of FALs in [12], and they provide the first examples of GFALs for which certain volume bounds in [11] are sharp. We conclude by describing one way in which nested links behave more like GFALs. We define a family of nested links whose longitude lengths are at most 4, yet with an unbounded number of crossing circles, a property shown to hold for GFALs in [10] but which does not hold for FALs; see Futer and Purcell [8].

2 Cell decompositions

In this section, we describe the standard cell decomposition on fully augmented links in detail, and we begin by introducing notation and terminology. Recall that a fully augmented link $\mathcal{F}$ is obtained from a twist-reduced link diagram of a link L in the plane $\mathcal{P}$ of projection. Around the twist regions place trivial components $C_1, \ldots, C_m$, called *crossing circles*, which are perpendicular to $\mathcal{P}$. Now remove all full twists from each twist region. The result leaves one or no crossings inside each crossing circle. The crossing circle is *flat* if there are no crossings (see Figure 1(a)), and *twisted* if there is one (see Figure 3(a)). The components of $\mathcal{F}$ coming from the original link L will be called *knot circles*. Each crossing circle C_i bounds a crossing disk D_i which is punctured twice by knot circles, making D_i a 3–punctured sphere in $M_{\mathcal{F}} = S^3 - \mathcal{F}$.

In this section, we describe the hyperbolic structure on $M_{\mathcal{F}}$ in detail. We use the cell decomposition of $M_{\mathcal{F}}$ found in the appendix of [9] and in [12], and call it the *standard cell decomposition* of $M_{\mathcal{F}}$. This decomposes $M_{\mathcal{F}}$ into two 3–cells with boundary, which are realized as right-angled ideal hyperbolic polyhedra. Some care is taken to describe the gluing instructions on these polyhedra, noting the differences that arise between flat and twisted crossing circles. None of the material in this section is new, but the following sections build on it, so it is included here for completeness.
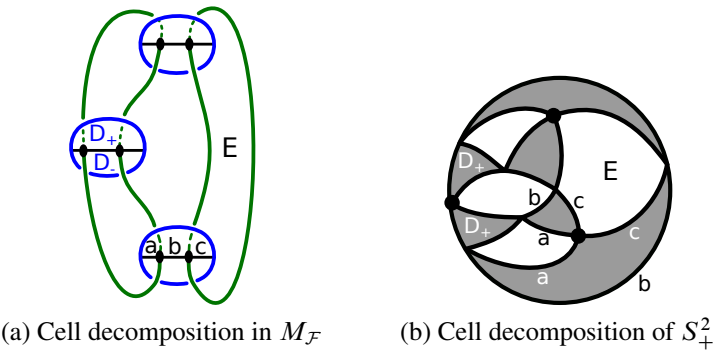
(a) Cell decomposition in $M_{\mathcal{F}}$ (b) Cell decomposition of S_+^2

Figure 1: The standard cell decomposition

Suppose $\mathcal{F}$ is a hyperbolic FAL with knot circles $K_1, \ldots, K_n$ and crossing circles $C_1, \ldots, C_m$. Initially consider the case where all the crossing circles are flat. The standard cell decomposition of $M_{\mathcal{F}}$ is constructed as follows; see [9; 12]. There are no 0–cells, so the resulting polyhedra will be ideal. The crossing discs D_i intersect the plane $\mathcal{P}$ in three segments each with endpoints on $\mathcal{F}$. The segments of intersection constitute the 1–cells, and representatives are labeled a, b and c in Figure 1(a). These 1–cells, together with the link $\mathcal{F}$, decompose the crossing discs D_i and projection plane $\mathcal{P}$ into the 2–cells. A 2–cell in $\mathcal{P}$ will be called a *planar* 2–*cell*, and the others will be referred to as *crossing* 2–*cells*. See Figure 1(a), where $D_{\pm}$ are crossing 2–cells and E is a planar 2–cell. The two 3–cells are the regions above and below the 2–cells, denote them by B_+^3 and B_-^3, respectively.

The standard cell decomposition of $M_{\mathcal{F}}$ induces one on the boundary of $B_{\pm}^3$, which we denote by $S_{\pm}^2 = \partial B_{\pm}^3$. We describe the induced decomposition on S_+^2 first. To see the decomposition on S_+^2, slice and flatten the top half of each crossing disk, getting two copies of the half disk and each 1–cell in the process. Portions of the link $\mathcal{F}$ form arcs in S_+^2, which are removed from S_+^2 since they are not in $M_{\mathcal{F}}$. Since removing an arc is topologically equivalent to removing a point, we shrink the missing arcs to missing points. The result is a cell decomposition of S_+^2, which we now summarize while adding some additional structure; see Figure 1(b).

The 0–cells are the (missing) points, which correspond to arcs of the link $\mathcal{F}$, and the 1–cells are two copies of each 1–cell in the standard cell decomposition of $M_{\mathcal{F}}$. There is one 2–cell on S_+^2 for each planar 2–cell, and each crossing 2–cell contributes two triangles to the decomposition (one for each side). Each (missing) vertex is 4–valent, and shading the triangles from the crossing 2–cells gives a checkerboard coloring
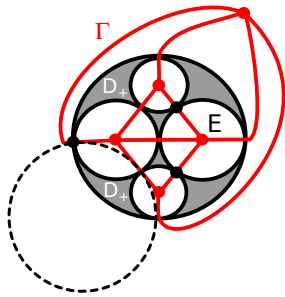
Figure 2: Circle packing from cell decomposition

of S_+^2. Thus every edge bounds a shaded triangle on one side and an unshaded region on the other. As in [12], we keep track of which (missing) vertices correspond to arcs of crossing circles by coloring them. The rest are not colored, and correspond to arcs of knot circles. Thus each triangle has one colored vertex, and each colored vertex is adjacent to the two shaded triangles corresponding to a given crossing disk.

The cell decomposition of S_+^2 can be realized as a circle packing, which is a first step toward realizing the topological space B_+^3 as a right-angled ideal hyperbolic polyhedron. As in [12] and Chapter 13 of [14], construct the *nerve* Γ of the cell decomposition of S_+^2 in the following way. Place a vertex in each unshaded region, and join two vertices of Γ with an edge where their corresponding regions meet at a (missing) vertex of the cell decomposition as in Figure 2. Since each shaded region is a triangle, the resulting nerve Γ is a triangulation of S_+^2. Invoking Andreev's circle packing theorem, there is a circle packing of the plane with Γ as its nerve. In our context, that means that the unshaded regions can be made circular, and the (missing) vertices become points of tangency between the circles. The edges of the cell decomposition become arcs of the circles joining points of tangency. The shaded regions are then "triangles" between three mutually tangent circles.

Now think of S_+^2 with its circular cell decomposition as the sphere of ideal points for $\mathbb{H}^3$, and we wish to construct an ideal polyhedron P_+ whose "footprint" is the circle-packing. The (missing) vertices of S_+^2, which are points of tangency between circles, will be the ideal vertices of P_+. To describe the faces of P_+, one observes that given any 2–cell in S_+^2, its vertices all lie on a circle. Indeed, any planar 2–cell in S_+^2 is unshaded, so by construction, its boundary is a circle of the circle-packing. Any crossing 2–cell is a shaded "triangular" region with exactly three vertices, which lie on a Euclidean circle (not one of the circle packing, but shown dotted in Figure 2). Thus given any 2–cell, its vertices are cocircular so they determine a hyperbolic plane in $\mathbb{H}^3$.

The face of P_+ corresponding to it is the ideal polygon determined by its vertices. The 1–cells are the hyperbolic lines of intersection between adjacent polygons. The interior of P_+ is all of $\mathbb{H}^3$ inside its faces.

To determine the dihedral angles along the edges of P_+, note that the dihedral angle between two intersecting faces of P_+ is the angle between their bounding circles at infinity. In general, the polyhedron determines whether you use the external angle or its supplement, but this will be irrelevant for us since all angles will be right angles. The boundary of a shaded face is the Euclidean circle through the points of tangency to three mutually tangent circles. This Euclidean circle is orthogonal to each of three mutually tangent circles, as is easily seen by sending one vertex to infinity. Thus the exterior angles between them, which are the dihedral angles between the faces of P_+, are right angles.

The cell decomposition on S_-^2 is identical to that on S_+^2 with the opposite orientation. In particular, each edge of the standard cell decomposition of $M_{\mathcal{F}}$ appears twice in it, and B_-^3 can be described geometrically as a right-angled ideal hyperbolic polyhedron P_-.

Remark The polyhedron P_- can be thought of as the hyperbolic reflection of P_+. Thus $M_{\mathcal{F}} = S^3 - \mathcal{F}$ decomposes into two identical right-angled ideal polyhedra, which can be checkerboard colored so that shaded faces are triangles. Such a decomposition will be important for the remainder of the paper.

When considering twisted crossing disks, the standard cell decomposition must be changed slightly. One still has a vertical crossing disk, but the other 2–cells aren't planar. As in Figure 3(a), the 1–cells near the crossing circle C_k are a, b and c, and we describe the 2–cells by listing their bounding arcs in order. The boundary of the 2–cell labeled W travels along the arc K_i in front of D_k, then right along the front of c, around the top semicircle of C_k, along the back of 1–cell a, and then continues back on the arc of K_j. Similarly, the boundary of the 2–cell Y travels along K_j in front, then left along the front of a, around the bottom semicircle of C_k, along the back of edge c, and continues back on the arc of K_i. Locally, the boundaries of X and Z consist of arcs of K_i (resp. K_j) in front of (resp. behind) D_k, together with the 1–cell b. This describes the standard cell decomposition of $M_{\mathcal{F}}$ near a twisted crossing circle.

We now determine the cell decomposition on $S_\pm^2$ near a twisted crossing circle C_k. For Figure 3, we consider both $S_\pm^2$ as the xy–plane in $\mathbb{R}^3$ together with the point at infinity

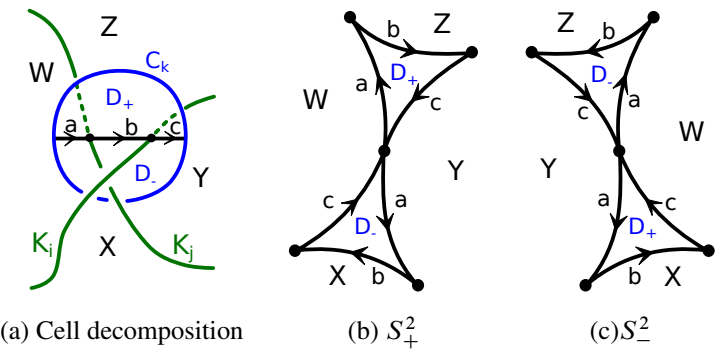Figure 3: The case of a twisted crossing disk

(a) Cell decomposition   (b) S_+^2 (c) S_-^2

and sketch the cell decomposition when viewed from infinity (or from inside $B_\pm^3$). Note that the bottom half D_- of D_k is visible from above the 2–cells in the front since the 2–cell W hides the top half D_+, while from behind, the top half D_+ is visible. The induced cell decomposition on S_+^2, after shrinking removed arcs to missing points, is as in Figure 3(b). Notice that the shaded triangles correspond to opposite halves of D_k, so do not get identified when gluing. A similar analysis produces the cell decomposition on S_-^2 pictured in Figure 3(c).

Combinatorially, then, the standard cell decompositions near a flat or twisted crossing disk are very similar. The difference is in the gluing instructions. For flat crossing disks, shaded triangles in the same polyhedron are identified, while for twisted crossing disks, one glues shaded triangles from opposite polyhedra.

3 Right-angled polyhedra

In the last section, we saw that the standard cell decomposition of a fully augmented link $\mathcal{F}$ produced two right-angled polyhedra $P_\pm$, together with gluing instructions, that describe the hyperbolic structure on $M_\mathcal{F}$. In this section, we allow slightly more general gluing instructions, and prove the result of the gluings is a complete hyperbolic manifold.

Taking our cue from FALs, we let P_+ be an ideal, right-angled, polyhedron whose faces can be checkerboard colored so that the shaded faces are triangular (these assumptions imply there is an even number of them). Now let r be the reflection across the hyperbolic plane disjoint from P_+, and let $P_- = r(P_+)$. We refer to a face F_+ of P_+ and its reflection $F_- = r(F_+)$ as *corresponding faces* and similarly for corresponding edges and vertices.

Definition 3.1 An *admissible* gluing pattern $\mathcal{A}$ on the polyhedra $P_{\pm}$ is one satisfying:

(1) Corresponding unshaded faces $F_{\pm}$ are identified by the composition of the reflection r followed by the reflection across the plane containing F_{-}.

(2) Corresponding shaded triangles $G_{\pm}$ are *not* identified.

(3) If $\varphi\colon G \to G'$ is the gluing map between shaded faces G and G', then $r \circ \varphi \circ r$ identifies their corresponding faces.

We say that an admissible gluing pattern *identifies corresponding faces correspondingly*. For unshaded faces, this means that corresponding unshaded faces are identified, as are their corresponding edges (as opposed to identifying faces with a twist). Identifying shaded faces correspondingly means that the gluing of G_{+} determines that of G_{-}.

We take a moment to interpret admissible gluings in the context of fully augmented links. In that setting, cutting along the standard cell decomposition creates the polyhedra $P_{\pm}$. In an admissible gluing, requiring that unshaded faces are identified is equivalent to gluing the planar 2–cells back together. This leaves a partially identified polyhedron with shaded triangles, which are halves of 3–punctured spheres, in its boundary to be glued. Requiring that corresponding shaded faces be glued correspondingly is tantamount to randomly pairing copies of 3–punctured spheres and gluing them. Thus, an admissible gluing starts with a fully augmented link, slices along crossing disks to produce a manifold with lots of 3–punctured spheres in its boundary, and reglues them in any order desired.

We show that admissible gluings produce hyperbolic manifolds.

Theorem 3.2 *The manifold $M_{\mathcal{A}}$ obtained by gluing the polyhedra $P_{\pm}$ according to an admissible gluing pattern $\mathcal{A}$ is a complete hyperbolic manifold.*

Proof To prove that the identifications in $\mathcal{A}$ result in a complete hyperbolic manifold, we first show that the gluing pattern is proper and then deal with completeness. To see that $\mathcal{A}$ is proper, note that there are no finite vertices on $P_{\pm}$, so we only need to check that the dihedral angles around edge-cycles add up to 2π.

Let a be an edge on P_{+}. Since the dihedral angle along any edge equivalent to a is $\frac{\pi}{2}$, we must show there are four edges in the edge cycle of a. The edge a bounds an unshaded face F_{+} on one side and a shaded triangle G_{+} on the other. The face F_{+} is glued to F_{-} so that a is identified with its corresponding edge $r(a)$. The face G_{+}

is glued to $G' \neq G_-$ via the isometry φ, identifying a and $\varphi(a)$. Let F' be the unshaded face that shares the edge $\varphi(a)$ with G'. Since F' in unshaded, it is identified with $r(F')$, producing a fourth edge identified with a. Finally, since the gluing pattern is admissible, $r(G')$ is glued to G_-, completing the edge cycle for a. Thus the angle sum around each edge is 2π.

Since an admissible gluing pattern is proper, $M_{\mathcal{A}}$ is a hyperbolic manifold. To prove that it is complete, we analyze the link of a vertex. Let v be a vertex of P_+ and L the link of v in $M_{\mathcal{A}}$. Furthermore, consider v to be ∞ in the upper half space model, and let S be a horosphere centered at ∞. Then $\pi_1(L)$ lifts to isometries of $\mathbb{H}^3$ that fix v and restrict to similarities on S. We wish to show the lift of $\pi_1(L)$ restricts to isometries of S by developing the link L in S.

Let F and F' be the unshaded faces of P_+ incident with v, and let H and H' be the planes containing them, respectively. Since P_- is the reflection of P_+, developing across faces F and F' corresponds to reflecting across H and H', respectively. Thus the copies of P_- attached to P_+ intersect S in rectangles congruent to that of P_+. Since further copies of $P_\pm$ in the unshaded direction are reflections across planes parallel to H and H', developing P_+ in the unshaded direction yields Euclidean congruent rectangles in S. In particular, the shaded dimension of the rectangles does not change as we develop in the unshaded direction.

Now let $\gamma \in \pi_1(L)$, and let φ_γ be the corresponding isometry. Then φ_γ restricts to a similarity on the horosphere S and can be realized as $\varphi_\gamma(z) = az + b$ for some constants $a, b \in \mathbb{C}$. Since the tessellation of S is rectangular, $a \in \mathbb{R}$, and φ_γ is a dilation followed by a translation. Develop P_+ to $\varphi_\gamma(P_+)$ first along unshaded faces, then along shaded faces. Since developing along the unshaded faces preserves the shaded dimension, as does developing along shaded faces, the shaded dimensions of P_+ and $\varphi_\gamma(P_+)$ are the same. Thus the dilation must be trivial, implying φ_γ restricts to an isometry of S, and the manifold $M_{\mathcal{A}}$ is complete. $\qquad\square$

The restriction that an admissible gluing $\mathcal{A}$ identifies corresponding unshaded faces correspondingly results in a totally geodesic reflection surface in $M_{\mathcal{A}}$. Manifolds containing such surfaces have interesting properties, some of which are outlined in [10; 11]. The process of changing the gluing pattern of a FAL to an admissible one is similar to Wielenberg's strategy for constructing manifolds sharing the same fundamental polyhedron; see [15].

There is a partial converse to Theorem 3.2. More precisely, let $P_\pm$ be ideal polyhedra constructed as above, and suppose a gluing pattern that identifies corresponding unshaded faces correspondingly yields a hyperbolic manifold. Under these conditions, the gluing instructions on shaded triangles must be admissible.

Lemma 3.3 *A hyperbolic gluing pattern on P which identifies corresponding unshaded faces correspondingly must be an admissible gluing pattern.*

Proof Let a be an edge of P_+ bounding unshaded face F_+ and shaded face G_+. Since the faces $F_\pm$ are identified, the shaded triangles $G_\pm$ cannot be, otherwise the angle sum around a would be π. Now let G' be the shaded triangle to which G_+ is glued via φ, and let F' be the unshaded face sharing edge $\varphi(a)$ with G'. Note that F' is glued to its corresponding face $r(F')$, which is adjacent to $r(G')$. To ensure the angle around a is 2π, we must glue $r(G')$ to the shaded triangle adjacent to F_-, which is G_-. Thus the gluing is admissible.   □

In this section, we started with polyhedra of the type found in FAL complements and showed that more general gluing patterns still result in complete hyperbolic manifolds. In the remainder of the paper, we topologically interpret various admissible gluing patterns.

4 Consecutive crossing circles

Several methods of creating new hyperbolic manifolds from old ones have been developed. Adams introduced the idea of a belt-sum of manifolds in [1] and used "walnuts" to construct hyperbolic manifolds with isometric cusps; see [3]. Furthermore, in [13], Ruberman has shown that mutants of hyperbolic knots are hyperbolic with the same volume. In this section, we focus on tangles involving consecutive crossing circles and introduce operations that maintain hyperbolicity while altering volume in a controlled fashion. Consecutive crossing circles occur in two ways, which we call parallel or series as indicated in Figure 4, each of which comprises a 6–tangle in a fully augmented link $\mathcal{F}$.

We introduce operations that replace the 6–tangles with ones that result in generalized fully augmented links. We refer to them as *surgeries* since, topologically, they result from cutting out a certain 6–tangle and pasting in a different one. Our goal is to show that the all the surgeries maintain hyperbolicity, and those of Figure 5 maintain volume while those of Figure 6 increase it by $2v_8$, where v_8 is the volume of a regular ideal octahedron. We proceed with formal definitions.
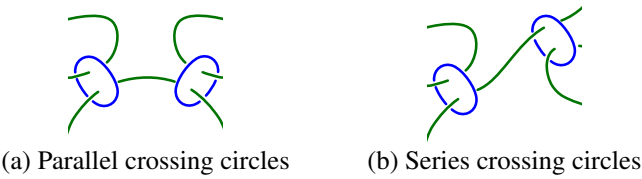
(a) Parallel crossing circles   (b) Series crossing circles
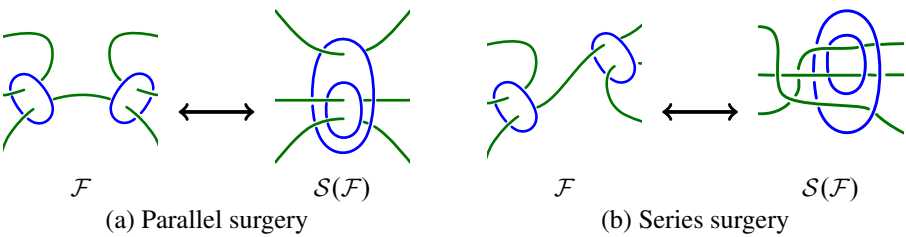
Figure 4: Consecutive crossing circles

$\mathcal{F}$ $\mathcal{S}(\mathcal{F})$ $\mathcal{F}$ $\mathcal{S}(\mathcal{F})$

(a) Parallel surgery   (b) Series surgery

Figure 5: Volume-preserving surgeries

$\mathcal{F}$ $\mathcal{S}(\mathcal{F})$ $\mathcal{F}$ $\mathcal{S}(\mathcal{F})$

(a) Parallel surgery   (b) Series surgery
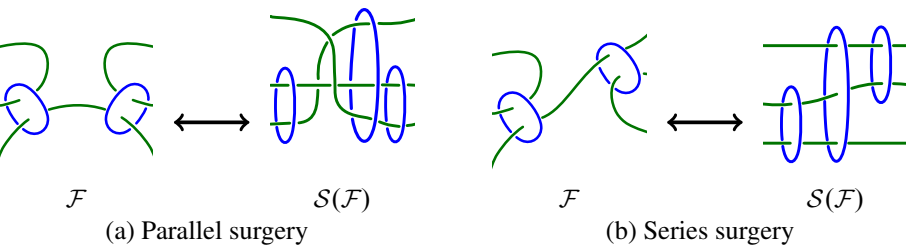
Figure 6: Volume-altering surgeries

(a)   (b)
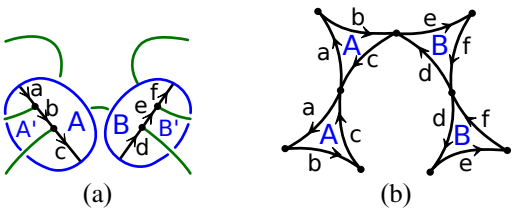
Figure 7: Cell decomposition and circle packing for $M_{\mathcal{F}}$

Definition 4.1 Let $\mathcal{F}$ be a hyperbolic fully augmented link with a 6–tangle containing consecutive crossing circles. A *volume-preserving surgery* on $\mathcal{F}$ replaces consecutive crossing circles with the corresponding tangle as in Figure 5. The resulting link is denoted by $\mathcal{S}(\mathcal{F})$. A *volume-altering surgery* replaces $\mathcal{F}$ with the link $\mathcal{S}(\mathcal{F})$ of Figure 6.

In general, volume-preserving surgeries are not mutations. Indeed, mutations preserve the number of components of a link while some volume-preserving surgeries do not, eg surgeries on Figure 1(a).

We begin by showing that volume-preserving surgeries are deserving of their title.

Theorem 4.2 *Volume-preserving surgeries, ie those in Figure 5, preserve hyperbolicity and volume.*

Proof The proof consists of noticing that minor changes in the gluing instructions for $P_\pm$ result in the desired surgeries. We treat the case of parallel crossing circles first. In this case, the circle packing described in Section 2 is as in Figure 7(b) where features with the same label are identified (the view from inside P_+ is shown, and that of P_- is its reflection). Now consider the gluing instructions as in Figure 8(b), which are the same as that of Figure 7(b) outside the local region pictured. It is a routine matter to verify that the gluings of Figure 8(b) constitute an admissible gluing, and Theorem 3.2 implies the result is a hyperbolic manifold (use corresponding gluings on P_-). Anticipating that it will be the complement of the surgered link $\mathcal{S}(\mathcal{F})$, we denote it by $M_{\mathcal{S}(\mathcal{F})}$ and proceed with the proof.

To show $M_{\mathcal{S}(\mathcal{F})} = S^3 - \mathcal{S}(\mathcal{F})$, we construct a cell decomposition of the complement of $\mathcal{S}(\mathcal{F})$ and show it results in the same polyhedra $P_\pm$ as $\mathcal{F}$ but with the altered gluing instructions. The crossing circles of Figure 8(a), together with one knot circle, bound a 3–punctured sphere intersecting the projection plane $\mathcal{P}$ in edges a, b and f. The inner crossing circle bounds a nested 3–punctured sphere intersecting $\mathcal{P}$ in edges c, d and e. These edges constitute the 1–cells. The crossing 2–cells above $\mathcal{P}$ are labeled A and B in Figure 8(a), while those under $\mathcal{P}$ are A' and B'. One readily verifies that the circle packing corresponding to this cell decomposition is that of Figure 8, demonstrating that $M_{\mathcal{S}(\mathcal{F})} = S^3 - \mathcal{S}(\mathcal{F})$.

Now consider the case of crossing circles in series, and observe that the circle packing is as in Figure 9(b). If one changes the gluing instructions as shown in Figure 9(d), note that the A faces on the same polyhedron have opposite orientation, so gluing them would result in a nonorientable manifold. Thus one glues faces from opposite polyhedra and checks that this is an admissible gluing, which results in a complete hyperbolic manifold by Theorem 3.2. To see that it is $M_{\mathcal{S}(\mathcal{F})}$, use the cell decomposition of Figure 9(c). The half-twist requires altering the 2–cells as in the case of twisted crossing circles for fully augmented links. After doing so, the polyhedra and gluing instructions are as desired. □

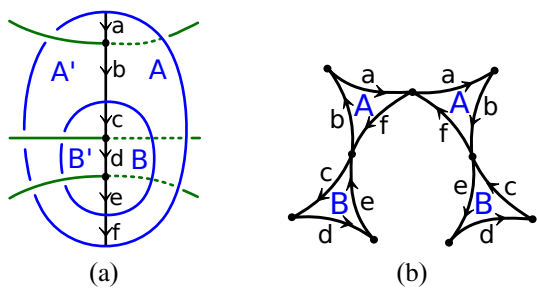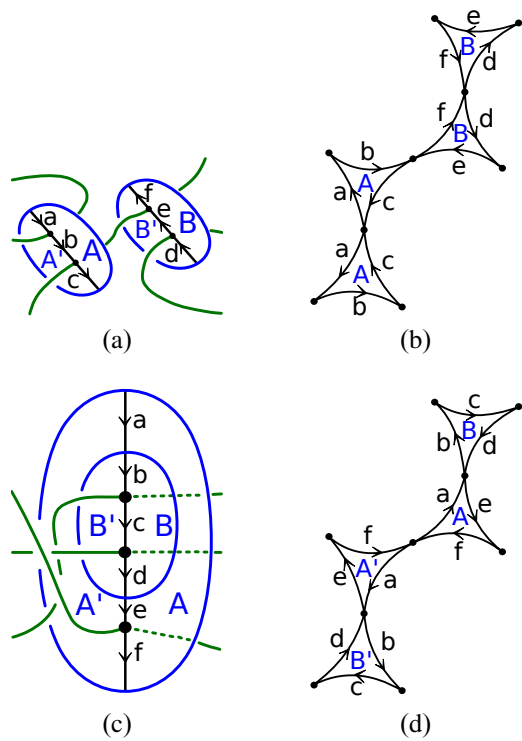Figure 8: Cell decomposition and circle packing for $M_{\mathcal{S}(\mathcal{F})}$

Figure 9: Series cell decomposition and circle packing

Remark One might expect the cell decomposition of $\mathcal{S}(\mathcal{F})$ to involve a 4–punctured sphere, corresponding to the larger crossing circle. This approach can be used, but the resulting polyhedra are not identical to those for $\mathcal{F}$, and the 4–punctured sphere is not totally geodesic. It is interesting to note that thinking of the crossing circles as nested 3–punctured spheres gives a cleaner picture of the geometry. This observation motivates the definition of nested links in Section 5.
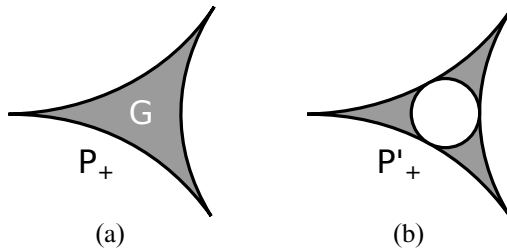
Figure 10: Appending a regular octahedron to P

Theorem 4.3 *Volume-altering surgeries, ie those in Figure 6, preserve hyperbolicity and change the volume by* $2v_8$.

Proof The first step is to describe a natural way to append a regular ideal octahedron to the polyhedra $P_\pm$; see Proposition 3.8 of [12] as well. Given a shaded triangle G in a circle packing bounded by three mutually tangent circles, one can form a fourth circle C which is tangent to each boundary arc of G. Color the interior of C white, and leave the three triangular components of $G - C$ shaded; see Figure 10. Thus one shaded triangle G is replaced by an unshaded circle and three shaded triangles. Notice that the circle C is tangent to exactly three others, and thus is a triangle as well.

Andreev's theorem implies this cell decomposition of S^2 can be realized as a right-angled ideal polyhedron which we label P'_+. We now demonstrate that P'_+ is obtained by appending a regular ideal octahedron $\mathcal{O}$ to P_+ by gluing one face to the shaded triangle G. After performing such a gluing, we refer to the face of $\mathcal{O}$ glued to G also by G, and we wish to show its circle packing is that of P'_+. Faces of $\mathcal{O}$ adjacent to G make right angles with it on the other side of G from P_+. Therefore, they are coplanar with the unshaded faces of P_+ that are adjacent to G, and the circle packing of P'_+ outside of G is the same as that of P_+. This accounts for four faces of $\mathcal{O}$ (the gluing triangle G and the three triangles that extend unshaded faces of P_+). The four remaining faces are the three shaded triangles and one unshaded circle of P'_+ inside the face G. Thus P'_+ is P_+ with a regular ideal octahedron added. Adding one to $r(G)$ on P_- results in P'_-.

The polyhedra $P'_\pm$ are obtained from $P_\pm$ by appending a regular ideal octahedron, and we now show that specific admissible gluing patterns on $P'_\pm$ yield the complements of the surgered manifolds in Figure 6. We treat the case of the series surgery in Figure 6(b) first. Append an octahedron to the interior copy of the shaded triangle B in P_+ with
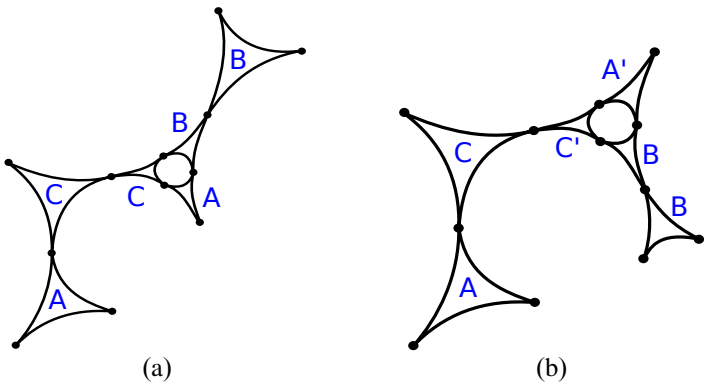
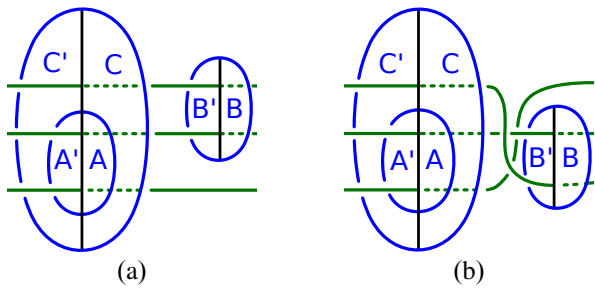Figure 11: Gluings corresponding to volume-increasing surgeries

Figure 12: Cell decompositions of volume-increasing surgeries

circle packing pictured in Figure 9(b), and append its reflection to P_-. The gluing patterns on P'_+ shown in Figure 11 can be reflected to give corresponding gluing patterns on P'_-. This implies that the additional corresponding unshaded triangles are glued correspondingly. Moreover, gluings outside the local region remain unchanged, so the pictured gluing pattern is seen to be admissible. Theorem 3.2 implies the gluing results in a complete hyperbolic manifold. The case of the parallel volume-altering surgery is pictured in Figure 11(b), and should be compared to Figure 7(b). The corresponding gluing instructions on P'_- are the reflections of those pictured, interchanging A and A', and the gluing is admissible resulting in a hyperbolic manifold.

To see that it is $M_{\mathcal{S}(\mathcal{F})}$, slide the 4–punctured sphere over the left 3–punctured sphere, and think of them as built from nested 3–punctured spheres as in the proof of Theorem 4.2; see Figure 12. The resulting cell decomposition on S^2_+ is shown in Figure 12, and the circle packing for this cell decomposition is readily seen to be that of $P'_\pm$ with the gluing instructions of Figure 11. □

We now study fully augmented links by composing these surgeries. In particular, we show in Corollary 4.5 that all octahedral fully augmented links can be obtained from the Borromean rings by a sequence of surgeries. We first recall some tools from [12]. Starting with a triangulation of S_+^2 (the nerve of the circle packing), Purcell colors edges so that each triangle has exactly one colored edge. The colored edges correspond to vertices on $P_\pm$, and the restriction that each face has exactly one colored edge means each shaded triangle on $P_\pm$ has exactly one colored vertex. Identifying two triangles which share a colored vertex results in a fully augmented link with flat crossing circles. Purcell shows that the fully augmented link is octahedral if and only if the triangulation you begin with is a central subdivision of K_4. It is natural, then, to compare fully augmented links whose corresponding triangulations of S_+^2 are related by a single central subdivision.

Theorem 4.4 *Let $\mathcal{F}$ and $\mathcal{F}'$ be fully augmented links whose corresponding colored triangulations are related by a single central subdivision. Then they are related by composing a volume-increasing surgery with a volume-preserving one.*

Proof Let $\mathcal{T}$ be a colored triangulation of S_+^2, and let $\mathcal{T}'$ be obtained from $\mathcal{T}$ by a central subdivision on a single face T. Extend the coloring of $\mathcal{T}$ to one for $\mathcal{T}'$ in the only way possible. The corresponding changes in circle packing are illustrated in Figure 10, where the face G corresponds to the triangle T being subdivided. When one subdivides the triangle T corresponding to the copy of A in the middle of Figure 13(a), one obtains the new gluing patterns pictured in Figure 13(b). We demonstrate that this gluing change is the composition of two surgeries.

There are two cases to consider, depending on which vertex of the shaded triangle C in Figure 13(a) is colored. If the top vertex is colored, then the crossing circles corresponding to the colored vertices are parallel, and the volume-increasing surgery of Figure 11(b) yields the gluing of Figure 14(b) with the appropriate change of labels. The top right portion of the gluing in Figure 14(b) is that of Figure 9(d) (replacing A and B of Figure 9(d) with D and C, respectively), so changing the gluing pattern to that of Figure 9(b) corresponds to a volume-preserving series surgery. The gluing pattern resulting from this change is that shown in Figure 13(b). Thus if the top vertex of C is colored, the central subdivision is realized by a parallel volume-increasing surgery followed by a series volume-preserving surgery. A similar analysis shows that if the bottom vertex of C is colored, the central subdivision is realized by a series volume-increasing surgery followed by a parallel volume-preserving surgery. □
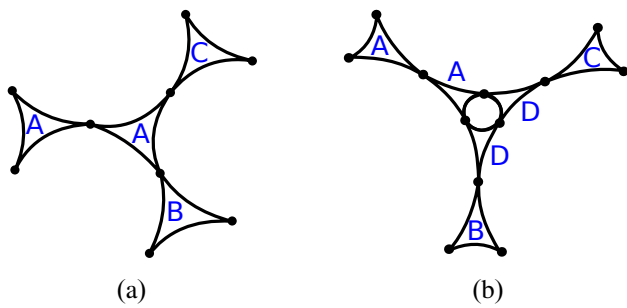
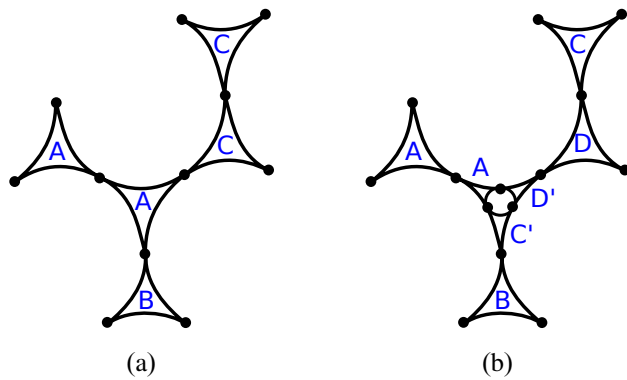Figure 13: Gluings corresponding to central subdivision

Figure 14: Geometrically composing surgeries

Corollary 4.5 *All octahedral fully augmented links can be obtained from the Borromean rings by a sequence of surgeries.*

Proof Purcell has shown that the nerve of any octahedral fully augmented link is a central subdivision of the complete graph on four vertices. By Theorem 4.4, it can be obtained from the link corresponding to a colored K_4 by a sequence of surgeries. Since any coloring of K_4 results in the Borromean rings, we are done. □

5 Nested links

In Section 4, we introduced surgeries on fully augmented links which resulted in links containing 4–punctured spheres. Thus these are examples of generalized fully augmented links whose geometric structure is similar to that of fully augmented links. Their geometry is best understood when the 4–punctured sphere is replaced with two 3–punctured spheres that share a puncture, ie that are *nested*. In this section, we

generalize the notion of nesting 3–punctured spheres to define a particular class of generalized fully augmented links which we call, appropriately, *nested links*. Crossing circles in nested links can bound n–punctured spheres, making them generalized fully augmented links whose geometry is closely related to that of fully augmented links.

We begin by defining nested links, and then use the dual Γ^* to the nerve Γ of the circle packing to characterize them in much the same way that Purcell used Γ^* to characterize hyperbolic fully augmented links. The main result of this section is Theorem 5.4, which determines the correspondence between certain spanning forests of Γ^* and hyperbolic nested links. Nested links then form a subclass of generalized fully augmented links whose geometry is very well understood.

Definition 5.1 Let $\mathcal{F}$ be a generalized fully augmented link. A *nesting* of a collection $\mathcal{C} = \{C_1, \ldots, C_m\}$ of crossing circles is an isotopy of $\mathcal{F}$ such that:

(1) It fixes the knot circles of $\mathcal{F}$, except near twisted C_i which carry their twist along.

(2) The collection $\mathcal{C}$ is made coplanar by the isotopy, with an outermost circle which we denote by C_1.

(3) The interior of C_1 decomposes into a collection of 3–punctured spheres by removing $C_2, \ldots, C_m$ and all knot circle punctures.

After the isotopy, the collection $\mathcal{C}$ is called *nested*.

Figure 12 illustrates a flat and a twisted nested collection with two crossing circles, and Figure 15 depicts more general cases. We refer to a nested collection as flat or twisted, as we did individual crossing circles, but with nested collections more complicated twisting can occur. Indeed, every crossing circle in $\mathcal{C}$ is the boundary of a 3–punctured sphere immediately interior to it, and each of those can either be flat or twisted. Our convention is that if a given crossing disc is twisted, the knot circles from one interior puncture cross those from the other, but those within a given puncture do not cross each other. Thus, in Figure 15(b), the crossing disks A and C are twisted while B and D are flat.

We make one final convention about twisting near a nested collection of crossing circles. If one starts with a generalized fully augmented link with lots of twisted crossing circles, then the isotopy to a given nesting can introduce full twists. We assume those are removed and only half-twists or no twists remain. This is analogous to the construction
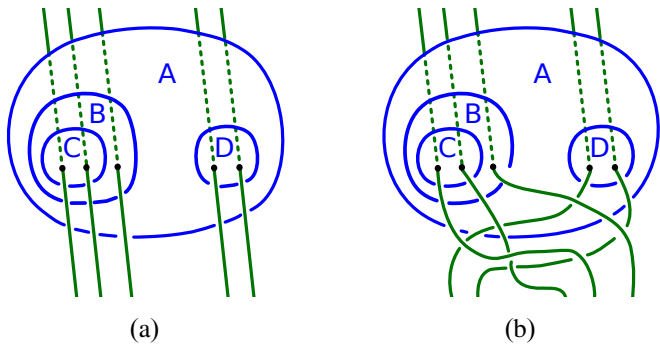
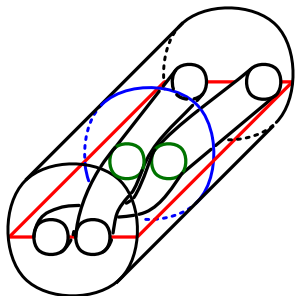Figure 15: Flat and twisted nested crossing circles

Figure 16: Nested annuli for the cell decomposition

for fully augmented links and is reasonable since the complements of the two links are homeomorphic.

Definition 5.2 A generalized fully augmented link is a *nested link* $\mathcal{N}$ if the crossing circles can be partitioned into collections which can be simultaneously nested.

The surgered links $\mathcal{S}(\mathcal{F})$ of Section 4 are examples of nested links. Note that the volume-altering surgeries result in links with at least two different nestings, obtained by pairing the 4–punctured sphere with the different 3–punctured spheres in the local tangle.

Given a hyperbolic nested link $\mathcal{N}$, one constructs the *nested cell decomposition* in much the same way as Section 2 describes the standard cell decomposition for fully augmented links. The crossing 2–cells for each nested collection all lie in the nesting plane, and the 1–cells are the intersection of these with the projection plane. The "planar" 2–cells are also constructed as for fully augmented links, with some care taken to account for the nesting. If a nested collection is flat, the planar 2–cells are indeed planar. If a nested collection is twisted, the planar 2–cells must follow the twisting.

More precisely, think of each crossing circle as the waist of an annulus, so the nesting of crossing circles yields nested annuli as in Figure 16. Outside these annuli, planar 2–cells really are planar. Between these annuli, one inserts 2–cells in the same manner as for flat or twisted crossing circles in Section 2. Taking care to have the 2–cells always attach to the intersection of the annuli with the projection plane $\mathcal{P}$ ensures that they extend through all nested annuli, and this results in a cell decomposition of the link complement.

Observe that the corresponding cell decomposition on $S_{\pm}^2$ has the same properties as that of a fully augmented link. Since each nested collection decomposes into 3–punctured spheres which are cut in half by the 1–cells, they yield triangles in the cell decomposition. Shading those triangles results in checkerboard colorings of the cell decompositions on $S_{\pm}^2$. The graph Γ whose vertices correspond to unshaded regions and whose edges correspond to vertices of the cell decomposition of $S_{\pm}^2$ is a triangulation, and Andreev's theorem leads to polyhedra $P_{\pm}$ as in Section 2. The dual Γ^* of Γ will be useful in characterizing nested links.

We now wish to demonstrate how to associate nested links with spanning forests of Γ^* which admit certain symmetries. Recall that vertices of Γ^* correspond to shaded triangles in the cell decomposition, while edges correspond to vertices of the cell decomposition of S_+^2. Since Γ is a triangulation of S^2, the dual Γ^* is a trivalent graph. In [12], Purcell shows that given such a graph, a choice of a spanning forest in which each component is an edge corresponds to a fully augmented link (Purcell calls this a *dimer* in [12, Section 2]). Indeed, the edges in the spanning forest correspond to the colored vertices of the cell decomposition of S^2 which, in turn, correspond to crossing circles in $\mathcal{F}$. The endpoints of an edge in the spanning forest correspond to shaded triangles of the cell decomposition which will be glued. Identifying shaded triangles from the same polyhedron, both in P_+ and P_-, results in a flat crossing circle, while gluing ones in opposite polyhedra result in a twisted crossing circle. In the case of fully augmented links, either choice results in a hyperbolic manifold.

We wish to generalize Purcell's construction to nested links by finding the appropriate generalization of a choice of dimer on Γ^*. A spanning forest comprised entirely of edges admits many symmetries. In particular, each edge of the forest has an involution that interchanges the endpoints. The appropriate generalization of a dimer turns out to be spanning forests in which each tree admits an involution. We introduce some terminology.

An *edge-preserving involution* f_e on a tree $\mathcal{T}$ is an involution of $\mathcal{T}$ which interchanges the endpoints of e. Clearly, not all trees admit edge-preserving involutions. An *edge-symmetric spanning forest* $\{\mathcal{T}_j, f_j\}$ is one in which an edge-preserving involution f_j is associated with each tree $\mathcal{T}_j$ of the forest. We now investigate the correspondence between edge-symmetric spanning forests of Γ^* and hyperbolic nested links. As a first step, we have:

Lemma 5.3 *A complete hyperbolic manifold can be associated with a spanning forest of Γ^* that is edge-symmetric.*

Proof   According to Theorem 3.2, we must show how to determine an admissible gluing pattern from an edge-symmetric spanning forest $\{\mathcal{T}_j, f_j\}$. Recall that for an admissible gluing on polyhedra $P_\pm$, corresponding unshaded faces are identified, and we must pair up noncorresponding shaded triangles. Since vertices of Γ^* correspond to shaded triangles on $P_\pm$, we can use the involutions f_j to pair shaded triangles. More precisely, let $v, f_j(v) \in \mathcal{T}_j$ correspond to the shaded triangles G and G', respectively. Then G and G' are not corresponding triangles since they are on the same polyhedron, so G can be paired with either G' or its reflection $r(G')$.

The tree $\mathcal{T}_j$ together with the involution f_j determine the gluing, and there are two cases to consider depending on whether v is a leaf of $\mathcal{T}_j$ or not. We require that edges paired under the involution f_j correspond to vertices of G and G' which are glued by the isometry. If v is a leaf of $\mathcal{T}_j$ which is the endpoint of edge e, then G can be paired with either G' or $r(G')$. To glue G and G', choose the orientation-preserving isometry φ that glues the vertex of P_+ corresponding to e to the vertex corresponding to $f_j(e)$ and such that $\varphi(P_+)$ is on the opposite side of G' from P_+. To identify G and $r(G')$, choose φ so that it identifies vertices on $P_\pm$ corresponding to edges e and $r(f_j(e))$ and so that $\varphi(P_+)$ and P_- are on opposite sides of $r(G')$. When every vertex is a leaf, these choices correspond to flat or twisted crossing circles, respectively.

If v is not a leaf, then there are at least two edges $e_1, e_2 \in \mathcal{T}_j$ incident with v. Let φ be the orientation-preserving isometry from G to G' which glues vertices corresponding to edges e_1, e_2 to those of $f_j(e_1), f_j(e_2)$. Then $\varphi(P_+)$ is either on the same or opposite side of G' from P_+. If $\varphi(P_+)$ and P_+ are on opposite sides, then use φ to glue G to G'. If they are on the same side, then glue G to $r(G')$ using the orientation-preserving isometry taking vertices corresponding to edges e_1, e_2 to those of $r(f_j(e_1)), r(f_j(e_2))$ (this can be realized by $r_{H'} \circ r \circ \varphi$, where H' is the hyperbolic plane containing $r(G')$). Note that in this last case where G is glued to $r(G')$, the

analogous reasoning on G' will glue it to $r(G)$ so that corresponding triangles are glued correspondingly.

For pairs of triangles on P_+ that get identified, glue their corresponding faces on P_- with the corresponding isometry. These choices determine an admissible gluing, which yields a complete hyperbolic manifold by Theorem 3.2.   □

Thus, according to Lemma 5.3, edge-symmetric spanning forests give rise to hyperbolic manifolds. Moreover, the proof also shows that the ambiguity is analogous to that of fully augmented links. More precisely, for each leaf of the forest, one can choose flat or twisted crossing circles. The remaining gluing instructions are completely determined by the given edge-symmetric spanning forest.

We now clarify the correspondence between edge-symmetric spanning forests and nested links. More precisely, we show that hyperbolic nested links give rise to edge-symmetric spanning forests in Γ^* and, conversely, the hyperbolic manifolds of Lemma 5.3 are complements of nested links in S^3.

Theorem 5.4 *Each hyperbolic nested link $\mathcal{F}$ gives rise to an edge-symmetric spanning forest of Γ^*. Conversely, each edge-symmetric spanning forest of Γ^* yields a hyperbolic nested link.*

Proof Let $\mathcal{F}$ be a hyperbolic nested link; we wish to associate with it an edge-symmetric spanning forest. We begin by demonstrating that each nested collection $\mathcal{C} = \{C_1, \dots, C_n\}$ determines an edge-preserving involution on a tree in Γ^*. Consider the situation for S^2_+, as that for S^2_- is analogous. Isotope the knot circles near $\mathcal{C}$ so that any twisting occurs on one side of the nesting plane and the knot circles on the other side are in the projection plane $\mathcal{P}$. On the flat side of the nesting plane, place a vertex in the top half of each crossing disc and connect the two vertices if their discs share a boundary component. The result is a tree, which is half of our desired tree. On the twisted side of the nesting plane, place a vertex in the top half of each flat crossing disc and the bottom half of each twisted crossing disc. Again, connect the vertices if their discs share a boundary component C_i, but if the vertices are on opposite sides, let the edge go through the intersection of C_i and $\mathcal{P}$ which misses the twisted 2–cells; see Figure 17. This forms a tree on the other side of the nesting plane which is isomorphic to the first. Connecting the vertices on opposite sides of the outermost 3–punctured sphere yields a single tree $\mathcal{T}$ that admits an edge-preserving involution. The involution interchanges vertices on opposite sides of the same 3–punctured spheres,

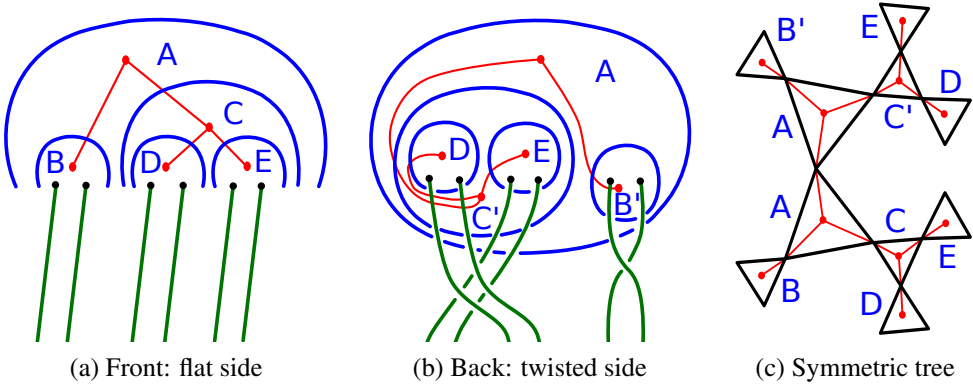(a) Front: flat side   (b) Back: twisted side   (c) Symmetric tree

Figure 17: Nested crossing circles induce $\{\mathcal{T}_j, f_j\}$.

and it interchanges edges through opposite sides of the same crossing circles. This is edge-preserving because it preserves the edge corresponding to the outermost crossing circle while interchanging its vertices. The image of $\mathcal{T}$ on S_+^2 is thus a subtree of Γ^* which admits an edge-preserving involution.

Now let $\{\mathcal{T}_j, f_j\}$ be the collection of subtrees of Γ^* corresponding to all nested collections $\mathcal{C}_j$ of crossing circles in $\mathcal{F}$. We claim $\{\mathcal{T}_j, f_j\}$ is a spanning forest. Indeed, since each shaded triangle of S_+^2 is in exactly one of the collections $\mathcal{C}_j$, the trees $\mathcal{T}_j$ are disjoint and span.

We now focus on the converse statement, that edge-symmetric spanning forests yield hyperbolic nested links. Lemma 5.3 shows that edge-symmetric spanning forests yield complete hyperbolic manifolds. It remains to show that these manifolds are complements of nested links in S^3.

Let $\{\mathcal{T}_j, f_j\}$ be an edge-symmetric spanning forest of Γ^*, and consider a fixed tree $\mathcal{T}$ of the forest. Let $\mathcal{T}_1$ be one component of $\mathcal{T}$ obtained by deleting the edge $e \in \mathcal{T}$ which is preserved by f. We let $\mathcal{T}_1$ represent the flat side of a nested collection $\mathcal{C}$. Let v be the endpoint of e contained in $\mathcal{T}_1$, and construct an outermost circle C_1 corresponding to v. For each edge in $\mathcal{T}_1$ adjacent to v, construct a crossing circle interior to C_1, and for each edge of $\Gamma^* - \mathcal{T}_1$ adjacent to v, construct a knot circle puncture interior to C_1. Make sure the constructed crossing circles and punctures are on the same sides (left or right) as the edges they correspond to. Repeat this process for all vertices in $\mathcal{T}_1$ to obtain a collection $\mathcal{C}$ of nested crossing circles and a flat side of knot circles.

Now use the gluing pattern determined by Lemma 5.3 to determine the twisting of the knot circles on the other side of $\mathcal{C}$. Start with flat knot circles, begin from the outermost

crossing circle, and work your way in. For each flat crossing circle, leave the strands of knot circles in the same order. For each twisted crossing circle with immediate interior crossing circles C_1 and C_2, introduce a half-twist between strands from C_1 and C_2 while leaving strands within them flat.

Repeat the above procedure for each tree in $\{\mathcal{T}_j, f_j\}$ to obtain collections $\mathcal{C}_j$ of nested crossing circles with knot strands that need to be glued. By construction, each end of a knot strand corresponds to an edge of $\Gamma^* - \mathcal{T}_1$. Connect ends of knot strands that correspond to the same edge. This can be done without introducing any further crossings since Γ^* is in S^2_+. The result is a nested hyperbolic link whose corresponding forest, given by the first statement in this theorem, is the original $\{\mathcal{T}_j, f_j\}$.   □

In [12] and [4], the authors point out that generalized fully augmented links usually have more complicated geometric structures. In particular, the standard cell decompositions are not totally geodesic and do not usually result in nerves that are triangulations. Using the nested cell decomposition, we find that nested links are a class of generalized fully augmented links which admit totally geodesic cell decompositions whose nerves are triangulations. This is one way in which nested links are GFALs which are similar to FALs.

Another similarity between nested links and FALs is that they provide examples of links for which certain volume bounds are sharp. In [11], Purcell bounds the volume of a GFAL in terms of the number of twist regions in a link diagram, generalizing the analogous bound found in [6] for FALs. In particular, it is shown that

$$\mathrm{vol}(S^3 - \mathcal{F}) \geq 2v_8(\mathrm{tw}(D) - 1),$$

where $\mathcal{F}$ is a GFAL obtained from a link L with diagram D, $\mathrm{tw}(D)$ is the number of twists in D, and v_8 is the volume of a regular ideal octahedron. Purcell notes in [11] that this bound is sharp for FALs, but comments that it appears "far from sharp" for GFALs. We show that, in fact, this bound is sharp for octahedral nested links, and thus for GFALs as well.

Theorem 5.5 *If $\mathcal{F}$ is an octahedral nested link, then*

$$\mathrm{vol}(S^3 - \mathcal{F}) = 2v_8(\mathrm{tw}(D) - 1).$$

Proof Since $\mathcal{F}$ is octahedral and its complement decomposes into two identical polyhedra, we know its volume is a multiple of $2v_8$. We must show that it is the

desired multiple. As $\mathcal{F}$ comes from fully augmenting a link diagram D, we see that $\mathrm{tw}(D) = c$, where c is the number of crossing circles in $\mathcal{F}$. The proof will follow from relating the number of vertices in Γ^* to both the number of octahedra and the number of crossing circles.

Let V denote the number of vertices in Γ^*; we first relate V to c. In the nested cell decomposition of a nested link, each crossing circle bounds a 3–punctured sphere interior to it, which is realized as four shaded triangles on $P_\pm$, two on each. Since shaded triangles correspond to vertices of Γ^*, we see that the number of crossing circles is half the number of vertices in Γ^*, so $c = \frac{1}{2}V$.

Now recall that the nerve Γ of an octahedral FAL is a central subdivision of the complete graph on four vertices; see [12]. Nested links share the same $P_\pm$ as FALs, so the same is true of nested octahedral links. Each central subdivision appends another regular ideal octahedron to each of $P_\pm$ and adds two triangles to the triangulation of S_+^2. Thus each central subdivision adds two vertices to Γ^*. We can now relate the number of octahedra in P_+ to V. One octahedron has four shaded triangles, so $\frac{1}{2}V - 1$ is the number of octahedra in P_+. Each central subdivision adds two vertices to Γ^* and one octahedron to P_+, so the number of octahedra in P_+ remains $\frac{1}{2}V - 1$.

Finally, since $\mathcal{F}$ is made from gluing $P_\pm$, there are twice as many octahedra in its complement, and we have

$$\mathrm{vol}(S^3 - \mathcal{F}) = 2v_8\left(\tfrac{1}{2}V - 1\right) = 2v_8(c - 1) = 2v_8(\mathrm{tw}(D) - 1). \qquad \square$$

Although nested links seem to behave more like FALs than GFALs, they are indeed GFALs. We conclude by introducing a family of nested links sharing a property with GFALs. Futer and Purcell [8] show that the length of longitudes of knot circles in hyperbolic FALs are bounded below by a linear function of the number of crossing circles. Purcell [10] shows that no such bound exists for GFALs. She does this by producing a family of GFALs with an unbounded number of crossing circles, but longitude length at most 4. We introduce a family of octahedral nested links with the same property, for which the proof of hyperbolicity is more elementary than that of the examples in [10]. Thus in this context, nested links behave more like GFALs than FALs.

Let $\mathcal{L}_n$ be the family of nested links described as follows. The knot circles are the closure of a half twisted n–braid, and the first crossing circle is the braid axis considered as a planar circle bounding an n–punctured disk. The crossing circles $C_2, \ldots, C_{n-1}$
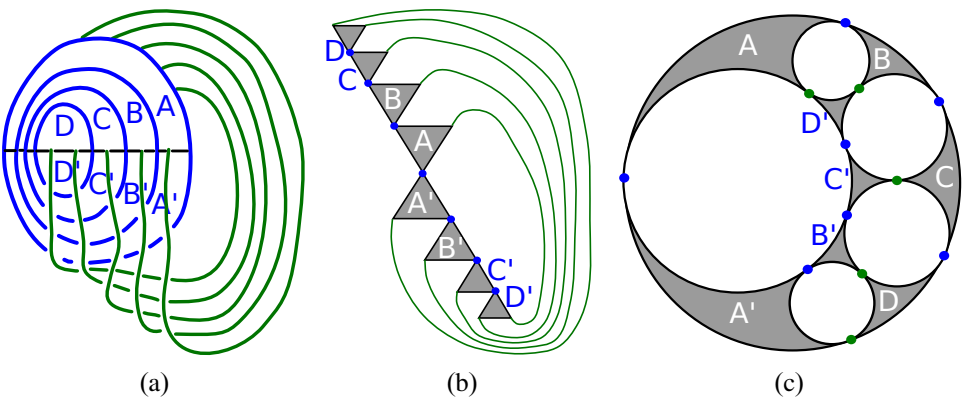
Figure 18: The link $\mathcal{L}_5$

are coplanar with C_1 and consecutively enclose one fewer braid strand until C_{n-1} encircles the first two strands; see Figure 18 for the link $\mathcal{L}_5$.

Lemma 5.6 *The link $\mathcal{L}_n$ is hyperbolic.*

Proof Figure 18(a) depicts the nested cell decomposition of $S^3 - \mathcal{L}_5$. The 1–cells are the horizontal edges, and the crossing 2–cells are the triangles A through D'. The planar 2–cells are half-twisted bands together with two disks corresponding to the innermost and unbounded regions of the projection plane. Figure 18(b) depicts the induced cell decomposition on S_+^2 before the knot circles have been shrunk to vertices but after shrinking the crossing circles. Figure 18(c) is the circle packing coming from the cell decomposition after shrinking the knot circles. The decomposition for general $\mathcal{L}_n$ is analogous, the only difference being more circles between the inner and outer ones. Note that this gives the same $P_\pm$ as a fully augmented 2–bridge link, just with different gluing instructions, and is therefore octahedral (see [10] for augmented 2–bridge link complement descriptions). Moreover, since the gluing pattern is admissible, Theorem 3.2 implies $\mathcal{L}_n$ is hyperbolic.   □

Theorem 5.7 *For $n > 3$, in the link $\mathcal{L}_n$, meridians of the knot circles have length 4 while longitudes are at most $4\sqrt{5}$.*

Proof There are two cases to consider, whether the knot circle goes once or twice through the nested crossing circles. The first case only occurs on the middle strand when n is odd, and we consider it now.
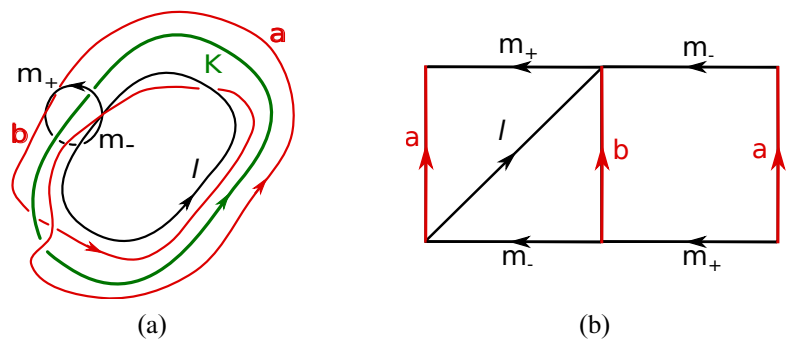
(a)   (b)

Figure 19: Cusp neighborhood of center knot circle

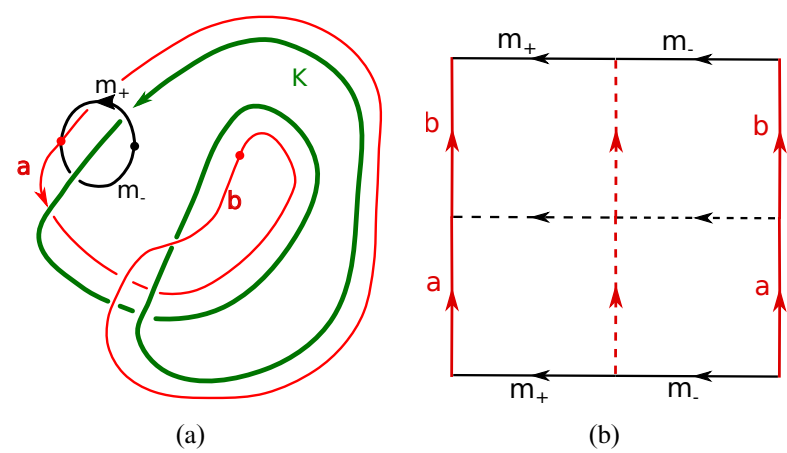(a)   (b)

Figure 20: Cusp of noncentral knot circle

Let K be the center knot circle, and consider the torus neighborhood pictured in Figure 19(a). The torus intersects the crossing 2–cells in two arcs, labeled $m_\pm$ in Figure 19(a), which comprise a meridian of K. Because of the half-twist, the planar 2–cells intersect the torus in two arcs, labeled a and b, which together with $m_\pm$ decompose the torus into two squares. One square is in P_+ and the other in P_-. A preferred longitude l of K crosses the square in P_+ diagonally from the beginning of arc a to the end of arc b.

This cell decomposition of the torus lifts to the universal cover of $S^3 - \mathcal{L}_n$. Assuming that infinity corresponds to the cusp K, the cell decomposition lifts to that of Figure 19(b), where the copies of $P_\pm$ have been identified along the unshaded face containing the

arc b. In the universal cover, copies of P_- are obtained by reflecting P_+ across unshaded faces, so ideal vertices corresponding to K lie directly beneath the arcs labeled $m_\pm$. Therefore, the most we can expand a horoball neighborhood about K is to the opposite side of a shaded face. Furthermore, this is the only obstruction since there is only one vertex corresponding to K in each of $P_\pm$ (in Figure 18(c), it is the vertex that faces C and C' share). If we assume this maximal expansion occurs at height 1, then the side of each square in Figure 19(b) has length 2. Thus the length of l is $2\sqrt{2}$ and the length of m is 4.

If the knot circle K goes twice around, then there are four vertices that correspond to it in $P_\pm$, two on each. For example, in Figure 18(c), the vertex shared by faces A and D' and that between A' and D correspond to one knot circle, while those shared by faces B, D' and B', D correspond to another. Thus the cell decomposition of a torus neighborhood of K lifts to four squares as in Figure 20(b), two in copies of P_+ and two in copies of P_-. Because of the half-twist in the cell decomposition of $\mathcal{L}_n$, the edges of the squares coming from the unshaded faces form a curve p in $S^3 - \mathcal{L}_n$ that has linking number 2 with K (the curve p is the concatenation of the two arcs a and b in Figure 20(a)). Additionally, the edges corresponding to shaded triangles form a meridian m. Thus a preferred longitude (linking number zero with K) is the curve $l = -2m + p$.

To calculate the length of l we consider a maximal cusp around K. As in the previous case, the most we can expand a horoball neighborhood about K is to the opposite side of a shaded face. In P_+, the two vertices corresponding to K are in different octahedra (for $n > 3$), so this maximal expansion can be achieved. If we assume this occurs at height 1, then the side of one small square has length 2. The length of $l = -2m + p$ is then $4\sqrt{5}$ and the length of m is 4.   □

In the case where $n = 3$, the knot circle K that goes twice around has meridian and longitude lengths $2\sqrt{2}$ and $2\sqrt{10}$, respectively. This is because the vertices in P_+ corresponding to K are opposite in the same octahedron (rather than distinct ones). If one assumes the squares of Figure 20 to have length 2, then the horoballs touch at height $\sqrt{2}$, so the lengths of curves must be adjusted.

References

[1] **C C Adams**, *Thrice-punctured spheres in hyperbolic 3–manifolds*, Trans. Amer. Math. Soc. 287 (1985) 645–656 MR

[2] **C C Adams**, *Augmented alternating link complements are hyperbolic*, from "Low-dimensional topology and Kleinian groups" (D B A Epstein, editor), London Math. Soc. Lecture Note Ser. 112, Cambridge Univ. Press (1986) 115–130 MR

[3] **C C Adams**, *Isometric cusps in hyperbolic 3–manifolds*, Michigan Math. J. 46 (1999) 515–531 MR

[4] **C Adams**, *Generalized augmented alternating links and hyperbolic volumes*, Algebr. Geom. Topol. 17 (2017) 3375–3397 MR

[5] **D B A Epstein**, **R C Penner**, *Euclidean decompositions of noncompact hyperbolic manifolds*, J. Differential Geom. 27 (1988) 67–80 MR

[6] **D Futer**, **E Kalfagianni**, **J S Purcell**, *Dehn filling, volume, and the Jones polynomial*, J. Differential Geom. 78 (2008) 429–464 MR

[7] **D Futer**, **E Kalfagianni**, **J S Purcell**, *On diagrammatic bounds of knot volumes and spectral invariants*, Geom. Dedicata 147 (2010) 115–130 MR

[8] **D Futer**, **J S Purcell**, *Links with no exceptional surgeries*, Comment. Math. Helv. 82 (2007) 629–664 MR

[9] **M Lackenby**, *The volume of hyperbolic alternating link complements*, Proc. London Math. Soc. 88 (2004) 204–224 MR With an appendix by Ian Agol and Dylan Thurston

[10] **J S Purcell**, *Slope lengths and generalized augmented links*, Comm. Anal. Geom. 16 (2008) 883–905 MR

[11] **J S Purcell**, *Hyperbolic geometry of multiply twisted knots*, Comm. Anal. Geom. 18 (2010) 101–120 MR

[12] **J S Purcell**, *An introduction to fully augmented links*, from "Interactions between hyperbolic geometry, quantum topology and number theory" (A Champanerkar, O Dasbach, E Kalfagianni, I Kofman, W Neumann, N Stoltzfus, editors), Contemp. Math. 541, Amer. Math. Soc., Providence, RI (2011) 205–220 MR

[13] **D Ruberman**, *Mutation and volumes of knots in S^3*, Invent. Math. 90 (1987) 189–215 MR

[14] **W P Thurston**, *The geometry and topology of three-manifolds*, lecture notes, Princeton University (1979) Available at http://msri.org/publications/books/gt3m

[15] **N J Wielenberg**, *Hyperbolic 3–manifolds which share a fundamental polyhedron*, from "Riemann surfaces and related topics: Proceedings of the 1978 Stony Brook Conference" (I Kra, B Maskit, editors), Ann. of Math. Stud. 97, Princeton Univ. Press (1981) 505–513 MR

Department of Mathematics, University of Virginia
Charlottesville, VA, United States

Department of Mathematics, University of Nebraska
Lincoln, NE, United States

Department of Mathematics, California State University
San Bernardino, CA, United States

jlh6fp@virginia.edu,   hayley.olson@huskers.unl.edu,   rtrapp@csusb.edu